Stem Cell Reviews and Reports (2018) 14:860–870
https://doi.org/10.1007/s12015-018-9831-z

The Transplantation of hBM-MSCs Increases Bone Neo-Formation and Preserves Hearing Function in the Treatment of Temporal Bone Defects – on the Experience of Two Month Follow Up

Lukáš Školoudík[1] · Viktor Chrobok[1] · Zuzana Kočí[2] · Jiří Popelář[3] · Josef Syka[3] · Jan Laco[4] · Alžběta Filipová[5] · Eva Syková[6] · Stanislav Filip[7]

Published online: 3 June 2018

Abstract

Temporal bone reconstruction is a persisting problem following middle ear cholesteatoma surgery. Seeking to advance the clinical transfer of stem cell therapy we attempted the reconstruction of temporal bone using a composite bioartificial graft based on a hydroxyapatite bone scaffold combined with human bone marrow-derived mesenchymal stromal cells (hBM-MSCs). The aim of this study was to evaluate the effect of the combined biomaterial on the healing of postoperative temporal bone defects and the preservation of physiological hearing functions in a guinea pig model. The treatment's effect could be observed at 1 and 2 months after implantation of the biomaterial, as opposed to the control group. The clinical evaluation of our results included animal survival, clinical signs of an inflammatory response, and exploration of the tympanic bulla. Osteogenesis, angiogenesis, and inflammation were evaluated by histopathological analyses, whereas hBM-MSCs survival was evaluated by immunofluorescence assays. Hearing capacity was evaluated by objective audiometric methods, i.e. auditory brainstem responses and otoacoustic emission. Our study shows that hBM-MSCs, in combination with hydroxyapatite scaffolds, improves the repair of bone defects providing a safe and effective alternative in their treatment following middle ear surgery due to cholesteatoma.

Keywords Temporal bone · Mesenchymal stromal cells · Scaffold · Osteogenesis · Ear function · Cholesteatoma

✉ Stanislav Filip
stanfil01@gmail.com

Lukáš Školoudík
lukas.skoloudik@fnhk.cz

Viktor Chrobok
viktor.chrobok@fnhk.cz

Zuzana Kočí
zuzana.koci@biomed.cas.cz

Jiří Popelář
jpopelar@biomed.cas.cz

Josef Syka
syka@biomed.cas.cz

Jan Laco
jan.laco@fnhk.cz

Alžběta Filipová
alzbeta.filipova1@gmail.com

Eva Syková
sykova@biomed.cas.cz

[1] Department of Otorhinolaryngology and Head and Neck Surgery, University Hospital, Hradec Králové, Czech Republic

[2] Department of Biomaterials and Biophysical Methods, Institute of Experimental Medicine, Czech Academy of Sciences, Prague, Czech Republic

[3] Department of Auditory Neuroscience, Institute of Experimental Medicine, Czech Academy of Sciences, Prague, Czech Republic

[4] The Fingerland Department of Pathology, University Hospital, Hradec Králové, Czech Republic

[5] Department of Radiobiology, University of Defence Brno, Faculty of Military Health Sciences , Hradec Králové, Czech Republic

[6] Institute of Neuroimmunology, Slovak Academy of Science, Bratislava, Slovak Republic

[7] Department of Oncology and Radiotherapy, Charles University, Faculty of Medicine, Hradec Králové, Czech Republic

Introduction

The management of middle ear cholesteatoma occasionally requires a canal wall down (CWD) mastoidectomy. This approach is highly effective in the treatment of cholesteatoma; however, this procedure often results in a modified external and middle ear anatomy; further, the ear canal loses its self-clearing ability and the exteriorized mastoid cavity becomes the target of chronic infections. Patients who have undergone this procedure need regular treatment, have bathing restrictions and difficult fitting for hearing aids. Some of these issues can be diminished using the obliteration technique [1, 2], which involves the reduction in size of the mastoid cavity but fails to preserve the anatomy of the external ear [3]. Despite the current advances in medicine a suitable biomaterial for the reconstruction of temporal bone defects, while maintaining the external ear canal and airy middle ear, is yet unavailable.

For more than a decade, stem cell research has received extensive attention in the field of bone tissue engineering due to their distinct biological capability to differentiate into osteogenic lineages, these cells are of varied origin and include embryonic stem cells (ESCs), bone marrow-derived mesenchymal stem cells (BM-MSCs), umbilical cord blood-derived mesenchymal stem cells (UCB-MSCs), adipose tissue-derived stem cells (ADSCs), muscle-derived stem cells (MDSCs), and dental pulp stem cells (DPSCs) [4, 5]. In this regard, human multipotent bone marrow derived mesenchymal stromal cells (hBM-MSCs) are primitive cells capable of restoring damaged mesenchyme and of differentiating into several cell lineages (e.g. osteocytes, chondrocytes, myocytes, adipocytes) [6, 7], thus it follows that MSCs are good candidates in regenerative medicine and cell based therapy in otorhinolaryngology [8–10] in combination with hydroxyapatite (Cem-Ostetic®), an osteoconductive material previously proven as suitable and promising in cell based therapy [5, 11, 12].

The regeneration process of MSCs involves either direct differentiation or the secretion of diverse growth factors and cytokines exerting a paracrine, protective effect on ischemic cells [13–15] by stimulating angiogenesis, limiting inflammation, suppressing apoptosis and recruiting tissue-specific progenitor cells [16, 17]. The latter is currently considered as responsible for their therapeutic potential [18–20]. Through their paracrine effect, MSCs have beneficial effects not only on anatomical and functional bone, but also on the surrounding soft tissue [10, 11].

Osteoconductive materials are commonly used in bone neo-formation; however, in a location such as middle ear, the efficacy of such construct is short-lived. In the present study we combined a commonly used osteoconductive biomaterial (Cem-Ostetic®) with hBM-MSCs to test their long-term efficacy in bone replacement in the middle ear, evaluating the effect of the combined biomaterial on the healing of post-operative temporal bone defects and the preservation of physiological hearing functions in a guinea pig model. The clinical evaluation, performed after 1 and 2 months of surgery, included animal survival, clinical signs of an inflammatory response, and tympanic bulla exploration. The radiological evaluation focused on bone defect reduction, new bone density, aeration of the middle ear, middle ear mucosa, and overall inner ear changes. The histopathological evaluation focused on osteogenesis, angiogenesis, and inflammation. hMSCs survival was evaluated by immunofluorescence. Hearing was evaluated by objective audiometric methods such as auditory brainstem responses and otoacoustic emissions.

The possibility of using human MSCs to improve bone healing without the necessity of long pre-cultivation on a scaffold prior to transplantation might simplify the treatment of such bone defects significantly, providing a viable alternative to traditional surgery [11, 12, 21]. Seeking to implement this stem cell therapy into clinical practice, we have conducted a study evaluating the safety and efficacy of a hydroxyapatite scaffold combined with hBM-MSCs in the treatment of bone defects following middle ear surgery in a guinea pig model.

Materials and Methods

Animals

A guinea pig model was chosen because of the considerable size of the tympanic bulla, ensuring wide access to the tympanic cavity [22]; more importantly, bone defects in the tympanic bulla are a suitable model reflecting an operation defect in the human mastoid cavity. For this purpose, thirty adult male guinea pigs, 240–410 g. in weight, were purchased and quarantined for 2 wk prior to the experiments (Lubos Sobota farm, Mestec Kralove; Czech Republic. License No. 28177/2009/17210). The animals were housed individually with access to food and fresh water ad libitum. Animal care followed the European Community Council and Czech Republic Directives guidelines (#86/609/EEC) and all experiments were performed with the approval of the Ethical Committee University Hospital and Medical Faculty Hradec Králové (authorization # 4/2013). All animals had normal eardrums without middle ear discharge at the beginning of the experiments.

Experimental Design

Three animals were used to introduce a surgical approach and optimization for biomaterial implantation, the remaining twenty seven animals were divided into three groups: One-month (1 M) experimental group ($n = 9$), two-month (2 M) experimental group (n = 9), and a control group (n = 9). The

experimental groups were implanted with the osteoconductive biomaterial Cem-Ostetic® (Berkeley Advanced Biomaterials, Inc.; CA, USA) combined with hBM-MSCs (MSC 3P suspended in 1.5 ml of Ringer's solution stabilized human albumin; Bioinova, Ltd. Czech Republic). The experimental groups 1 M and 2 M were analysed at 30 and 60 days, respectively, after implantation of the composed biomaterial (Fig. 1a, b). The control group was implanted only with the osteoconductive biomaterial Cem-Ostetic® and analysed after 30 days. Following surgery, all animals were treated with a daily 10 mg/kg dose of cyclosporine A, an immunosuppressor drug (CSA; Sandimmune Neoral, Novartis, Germany). At the end of the experiment (day 30/60 after surgery), the animals were euthanized by intraperitoneal injection of 100 mg/kg ketamine hydrochloride (Gedeon-Richter, Hungary) and 10 mg/kg of xylazine hydrochloride (Interchemie Gasternory, Holland) followed by transcardial perfusion with 10% formaldehyde (Sigma-Aldrich; MO, USA).

Surgery

Guinea pigs were anesthetized with 50 mg/kg ketamine hydrochloride (Gedeon-Richter, Hungary) and 5 mg/kg xylazine hydrochloride via *i.m.* injection (Interchemie Gasternory, Holland). An anterior surgical approach to the left tympanic bulla was chosen. After submandibular skin incision, the anterior surface of the tympanic bulla was exposed. A 4 mm diameter puncture was created using a micro dissector and small forceps. Middle ear ossicles and the tympanic membrane were preserved. The puncture was covered with the biomaterial and the wound closed with a single layer of 3–0 Safil suture. The animals were treated with *i.m.* 4 mg/kg carprofen (analgesic) (Janssen Pharmaceutica NV, CCPC, Belgium) and 10 mg/kg enrofloxacine (antibiotics) (eBioscience; CA, USA) at the end of the surgery.

Cell Preparation

Bone marrow was obtained from the iliac crest of healthy donors with informed consent (Ethical Committee of Institute Experimental Medicine, Academy of Science in Prague) and processed in a clean room facility of Bioinova, Ltd. In brief, bone marrow was mixed with Gelofusine® (B. Braun, Melsungen AG, Germany) and the mononuclear fraction collected and cultured on plastic flasks at a density of 70,000–140,000 cells/cm^2 (TPP Techno Plastic Products AG; Trasadingen, Switzerland). Non-adherent cells were removed after 24 and 48 h by replacing the media. The adherent cells were further incubated at 37 °C in a humidified atmosphere containing 5% CO_2 in enriched MEMAlpha (Lonza Walkersville Inc.; MD, USA) media containing 5% platelet lysate (Bioinova, Ltd. Czech Republic) and 10 μg/ml gentamicin (Gentamicin Lek®; Lek Pharmaceuticals, Ljubljana, Slovenia). The media was replaced twice per week. MSCs were identified according to their spindle-shaped morphology and adherence capacity, with their phenotype later confirmed by flow cytometry (FACSAria; BD Biosciences, CA, USA) using the markers: lin$^-$/CD105$^+$/CD73$^+$/CD90$^+$. To assess the differentiation potential of these MSCs, the cells were differentiated into osteogenic, chondrogenic and adipogenic lineages using standard differentiation media [23]. Cell viability (≥95%) was evaluated using trypan blue staining, and the cultures were tested for bacterial or fungal contamination. Afterwards, a cell suspension containing 20×10^6 of hBM-MSCs 3P (3rd passage) was then greenlit for transplantation into temporal bone defects in guinea pigs.

Scaffold Preparation

Hydroxyapatite (Cem-Ostetic®; Berkeley Advanced Biomaterials, CA, USA) was used as an osteoconductive

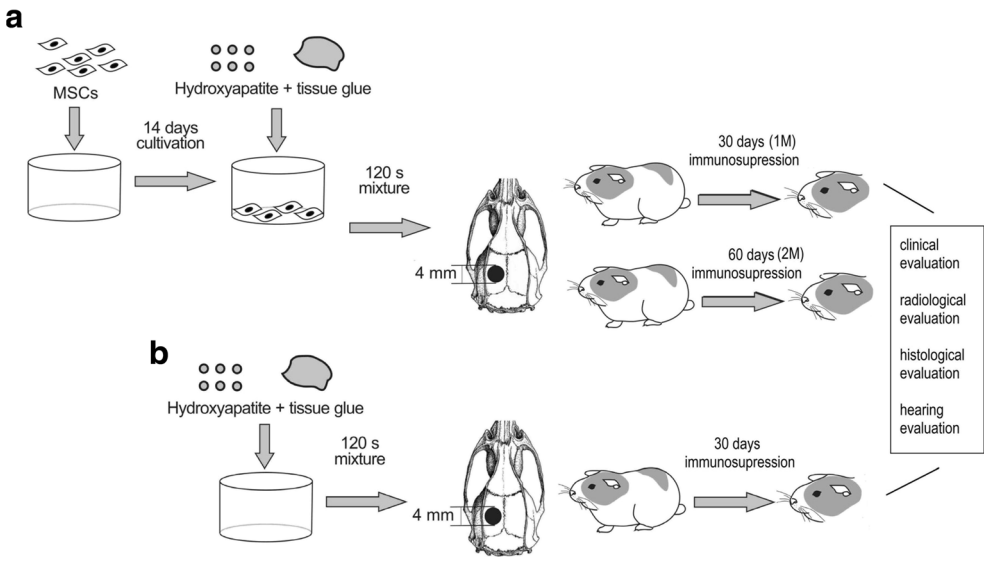

Fig. 1 Schematic diagram of the experimental protocol. The biomaterial seeded with hBM-MSCs implanted into the bone defects of Guinea pigs (**a**) was analysed after one (1 M) and two (2 M) months of surgery; the control group was implanted with the scaffold only (**b**)

material carrying hMSCs. Thanks to its chemical similarity with organic bone [Ca_{10} $(PO_4)_6$ $(OH)_2$], the material has excellent biocompatibility and proved as a suitable scaffold for osteogenic cells. A 1 cm^3 section of synthetic bone graft was covered with 100 mg of tissue glue (Tisseel Lyo, Baxter Czech; Prague, Czech Republic) and seeded with 1.6×10^6 hBM-MSCs. Each osteogenic scaffold was implanted according to their suitability to the created bone defect. Osteogenic scaffold implants lacking hBM-MSCs were used for the control group.

Radiological Evaluation

Radiological examination was performed using a 128-row multi-detector Computed Tomography (CT; SIEMENS SOMATOM Definition AS/AS_+) with a HRCT (high resolution computed tomography) reconstruction algorithm. Source data collimation was of 0.625 mm, table feed was 4 mm/s, coronal plane reconstructions were obtained, slice thickness 0.4 mm, FOV 55 X 55 mm, matrix 512 X 512, images were evaluated in window centre 700 HU and window width 4000 HU.

Histopathological Evaluation

The temporal bone specimens were fixed in 10% neutral formalin (Sigma-Aldrich; MO, USA) for 24 h and gently decalcified with 5% formic acid (Sigma-Aldrich; MO, USA) for 5 days. The tissue was embedded in paraffin, cut into 4 μm-thick sections, and stained with haematoxylin (Sigma-Aldrich; MO, USA) and eosin (Junsei Chemicals, Tokyo, Japan); or H&E and Masson's trichrome (TRI) (MT, Sigma-Aldrich; MO, USA). In addition, each sectioned was stained with chloroacetate esterase (CHAE) (MT, Sigma-Aldrich; MO, USA) according to standard histochemical protocol. The structural changes in the middle and inner ear were evaluated in the H&E stained sections. For the immunohistochemical analysis, the sections were mounted on slides coated with 3-aminopropyltriethoxy-silane, deparaffinised in xylene, and rehydrated in descending grades of ethanol (100–70%) (all reagents: Sigma-Aldrich; MO, USA). The following antibodies were used: anti-CD3 (polyclonal, 1:200), anti-CD20 (L26, 1:300), anti-CD31 (JC70A, 1:50), anti-CD68 (PG-M1, 1:50), and anti-TRAP (ab58008, 1:750); all antibodies were purchased from Dako (Glostrup, Denmark), except for TRAP (Abcam, Cambridge, United Kingdom). TRAP staining was done manually, as follows: for antigen retrieval, the tissue was processed in the microwave vacuum histoprocessor RHS 1 (Milestone; Sorisole, Italy) at 97 °C/pH 6.0 for 4 min. Endogenous peroxidase activity was quenched using 3% hydrogen peroxide (MT; Sigma-Aldrich). After incubation with the antibodies, the sections were subjected to EnVision+ Dual Link System-HRP (Dako, Denmark). Finally, the sections were stained with 3–3′-diaminobenzidine (DAB) and counterstained with H&E. The staining with the remaining antibodies was performed using a immunostainer BenchMark Ultra (Roche, Basel, Switzerland), with Ultra View Universal DAB Detection Kit and Bluing Reagent as the visualization reagent and chromogen (all reagents: Roche, Basel, Switzerland). Appropriate positive and negative controls were used. All the samples were evaluated by a pathologist in a blind study. The zone with the implanted material was examined for inflammatory response as well as for new bone formation using a light microscope. Specifically, the numbers of CHAE-positive neutrophils, eosinophils, $CD3^+$ T-lymphocytes, $CD20^+$ B-lymphocytes in three high power fields (HPFs) (10× eyepiece and 40× objective; area 0.152 mm^2) were counted in the areas in which the inflammation was most intense. The presence of $CD68^+$ and TRAP-positive cells was also examined. Using the NIS Elements AR 3.0 program, new bone formation was calculated as the ratio:

$$\frac{\text{total area of newly formed bone trabeculae}}{\text{total area of the implation zone}}$$

Immunofluorescent Microscopy

The temporal bone samples were embedded in paraffin after decalcification and cut into 4 μm-thick sections. The primary antibody against human cytochrome C oxidase subunit II – (MTCO2, 1:250) (Ab3298; Abcam, Cambridge, UK) targets human cells only. Anti-collagen I (COLL1, 1:500) (Ab90395; Abcam) was used to detect new bone formation. A secondary AlexaFluor 488 conjugated antibody was used for fluorescent detection (1:200) (a11029, Molecular Probes; OR, USA). All samples were evaluated by two independent observers (Z.K and B.S.). The zone with the implanted material was close to the middle ear cavity and examined for positive MTCO2 and COLL1 under a light (Leica CTR 6500; Leica Microsystems, Wetzlar, Germany) and confocal microscopes (Zeiss LSM 5 DUO, Carl Zeiss, Jena, Germany).

Hearing Function Test

The hearing function of guinea pigs in the 2 M experimental group was tested in a sound proof and anechoic room, with pre and postoperative testing 2 mo after bilateral surgery. The guinea pigs presenting ear discharge, tympanic membrane perforation, or inflammatory thickness were excluded.

Hearing Threshold

The hearing threshold in guinea pigs was assessed by auditory brainstem responses (ABRs). The guinea pigs, previously anesthetized with an *i.m.* injection of 50 mg/kg ketamine

(Narkamon 5%, Spofa) and 8 mg/kg xylazine (Sedazine, Fort Dodge), had their ABRs recorded by three stainless-steel needle electrodes placed sub dermally over the vertex (active), and right/left mastoids (reference and ground electrodes) of the animal. The signal from the electrodes was amplified by a TDT RA16PA RA4LI preamplifier and processed with a TDT data acquisition system RX5–2 Pentusa Base Station (Tucker-Davis Technologies, Gainesville, FL, 16-bit A/D converter, sampling rate 50 kHz) using BioSig software. The acoustic stimuli for the ABR recordings were generated by a PC-based TDT system, presented in free-field conditions via ribbon tweeter RAAL 70-20XR and mid-bass woofer Selenium 6W4P, placed 70 cm in front of the animal's head. Pure tone pip stimuli, duration 5 ms, 2-ms rise/fall times, frequency range 1–32 kHz, presented in one octave steps with decreasing intensity by 5 dB steps were used to assess the hearing threshold. The frequency thresholds were determined as the minimal tone intensity evoking a visually noticeable potential peak in the expected time window of the recorded signal. Most frequently, the ABR wave III was taken as dominant in determining the hearing threshold.

Distortion-Product Otoacoustic Emission

To test the physiological status of the outer hair cells in the cochlea, the distortion-product otoacoustic emissions (DPOAEs) were recorded with a low-noise microphone system (Etymotic probe ER-10B+; Etymotic Research, Elk Grove Village, IL, USA). DP-grams (the function of the DPOAE amplitude relative to noise level on an increasing stimulus frequency) were recorded with a four points per octave resolution over the 1–38 kHz frequency range. The acoustic stimuli (two primary tones with frequency ratio F2/F1 = 1.21 and level L1 = L2 = 65 dB) were generated by a TDT System III (RP2 processor; sampling rate 100 kHz) and presented to the ear canal with a custom-made piezoelectric stimulator connected to the probe with 10-cm-long silastic tubes. The signal from the microphone was analysed with a TDT System III (RP2 processor; sampling rate 100 kHz). DPOAEs were measured consecutively in both ears.

Statistical Analysis

Numerical results obtained from an Equal-Variance T-Test (software NCSS9) are expressed as mean values ± SEM (Standard error of the mean), where $p \leq 0.05$ was considered significant. The hearing tests, evaluated by distortion-product otoacoustic emission (DPOAE), were processed by one-way ANOVA with Bonferroni post hoc test ($p \leq 0.05$). All statistical analyses were performed by a certified statistician.

Results

Clinical Evaluation

For the clinical evaluation, 8 animals from both control and 1 M groups were available (the missing animals died as a result of operative trauma); the 2 M group could be analysed in its entirety (9 animals). Neither signs of ear discharge nor post-operative vestibulopathy were present. Macroscopic exploration of the tympanic bulla proved firm occlusion of the operative defect in the anterior wall of the bulla in all cases (Fig. 2a–b). No inflammatory response occurred around the site of the implanted material.

Histopathological Evaluation

Osteogenesis The pathologist was able to identify the zone of implanted material and osteogenesis in all 25 temporal bones analysed (Fig. 3a–c). The mean ratio of new bone formation, in 1 mm^2 of implanted material, was of 258,144 μm^2 in the control group, whereas in the experimental group 1 M the mean ratio of new bone formation increased significantly to 616,846 μm^2 ($P_1 = 0.0047$) and to 808,172 μm^2 in the 2 M group; the latter value was statistically significant when compared to the control group ($P_2 = 0.0019$) but not to the 1 M group ($P_3 = 0.0654$). The volume percentage of new immature bone was calculated in the temporal bone defect, where the control group presented only 22% of new immature bone; on the other hand, new immature bone formation increased significantly to 62% in the 1 M group ($P_1 = 0.0172$) and to 81% in the 2 M group, where the difference was statistically significant when compared to the control group ($P_2 = 0.0098$) but not to the 1 M group ($P_3 = 0.0696$) (Table 1).

Angiogenesis Angiogenesis could be observed in all groups. In the control group, the mean number of small blood vessel lumina was 9 (SEM ± 4.2), 13 (SEM ± 6.4) in the 1 M group, and 7 (SEM ± 5.2) in the 2 M group. No significant difference was appreciated in any case (Table 1).

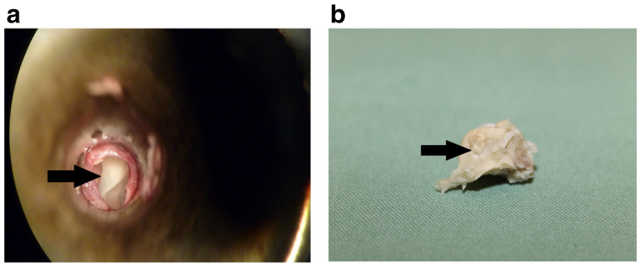

Fig. 2 Left tympanic bulla surgery. The arrow marks the surgical defect of the tympanic bulla (Ø 4 mm) (**a**). Tympanic bulla 30 days after implantation, the arrow marks the osteointegration of the biomaterial seeded with hBM-MSCs (**b**)

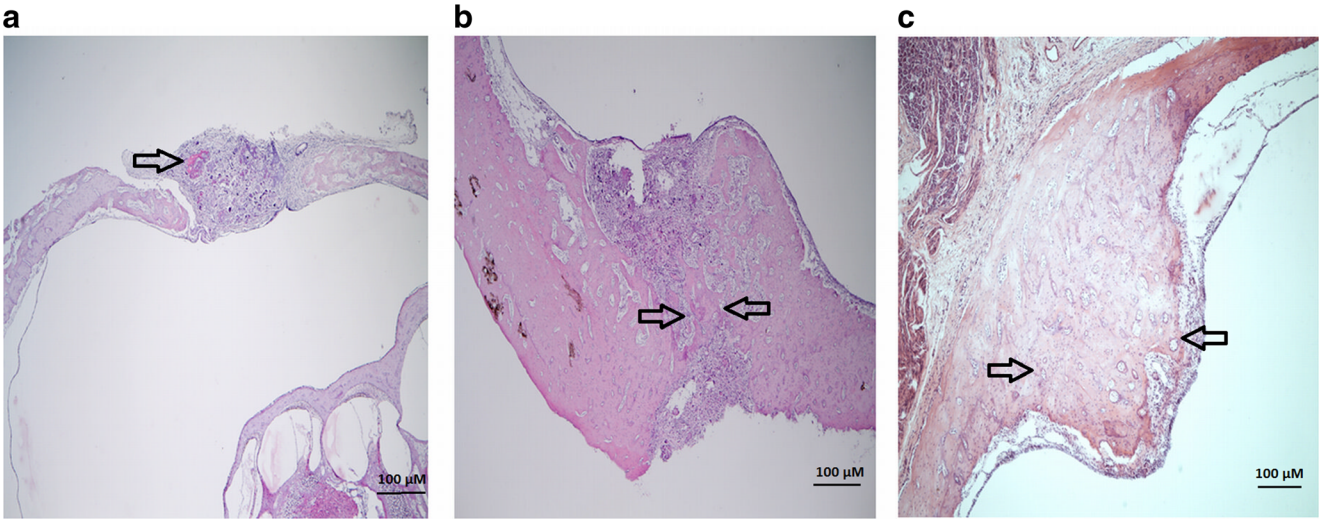

Fig. 3 Histological evaluation of the implant or control zones. Newly formed bone trabeculae (black arrows) are in direct contact with hydroxyapatite (seen as a bubbly greyish material). The amount of osteoid between control samples (**a**) and the samples with hBM-MSCs – experimental groups 1 M (**b**) and 2 M (**c**) - were analysed and compared. Haematoxylin-eosin staining; scale bar 100 μm

Inflammation After surgery, the immunohistochemical examination revealed the presence of $CD3^+$ T-lymphocytes in all groups, measured as cells/HPF (high-power field = 0.152 mm^2). In the control group, the mean number of $CD3^+$ T cells was of 26 (SEM ± 12,4); however, $CD3^+$ cell infiltration was higher in the 1 M group with a mean number of 65 (SEM ± 11,9) ($P_1 = 0.0140$) whereas in the 2 M group $CD3^+$ infiltration decreased, showing a mean number of 16 (SD ± 8,1) T-lymphocytes per HPF ($P_2 = 0.1730$) (Table 1).

$TRAP^+$ macrophages were observed in all samples. Immunohistochemical analysis revealed no CHAE-positive neutrophils, $CD20^+$ B-lymphocytes or $CD68^+$ cells (Table 1).

Histology of Inner Ear

The histological examination did not show any structural abnormalities of the cochlea in any of the 25 specimens. The Reissner's membrane separated the cochlear duct from the scala vestibuli in all specimens with normal stria vascularis

Table 1 Histomorphological analysis of new bone formation at the site of the tympanic bulla lesion at 30 and 60 days after surgery in the 1 M and 2 M groups, transplanted with osteoconductive material (CEM-OSTETIC ®) seeded with 5×10^6 cells hBM-MSCs, and in the control group. Data shown describe the mean ratio ± SEM. P_1 - control vs 1 M; P_2 - control vs 2 M; P_3 - 1 M vs 2 M. $p \leq 0.05$ was considered to be significant

	Control group (mean values ± SEM)	Experimental group (mean values ± SEM)		Statistical significance
		1 month (1 M)	2 month (2 M)	
New bone formation (μm^2 in 1 mm^2)	258,144 (SEM ± 21,018.5)	616,846 (SEM ± 17,757.3)	808,172 (SEM ± 14,650.3)	$P_1 = 0.0047$ $P_2 = 0.0019$ $P_3 = 0.0654$
New bone formation (volume %)	26 (SEM ± 1.2)	62 (SEM ± 1.8)	81 (SEM ± 1.5)	$P_1 = 0.0172$ $P_2 = 0.0098$ $P_3 = 0.0696$
Angiogenesis ($CD31^+$ cells in 0,283 mm^2)	9 (SEM ± 4.2)	13 (SEM ± 6.4)	7 (SEM ± 5.2)	P_1; P_2; P_3 NS
CD^3 cells (T-lymphocytes in 0.152 mm^2)	26 (SEM ± 12.4)	65 (SEM ± 11.9)	16 (SEM ± 8.1)	$P_1 = 0.0140$ $P_2 = 0.1730$ $P_3 = 0.0063$
CHAE positive neutrophils	0	0	0	
$CD20^+$ cells (B-lymphacytes)	0	0	0	
$CD68^+$ cells (macrophages)	0	0	0	

appearance along the outer wall of the cochlear duct. The organ of Corti was observed with intact basilar membrane and vital neuroepithelium in all cases (Fig. 4).

Immunofluorescent Microscopy

MTCO2 positive human cells were observed in both 1 M and 2 M experimental groups, estimating an 88% cases (7 from 8 specimens) for the former and 67% cases (6 from 9 specimens) for the latter (Fig. 5). In all cases, newly formed collagen was detected within the implant with COLL1 staining.

Hearing Tests

Hearing capacity was evaluated in the 2 M experimental group; however, one Guinea pig was excluded from the ABR and DPOAE evaluations because of tympanic membrane thickness, as observed on a CT scan.

Hearing Thresholds

The hearing thresholds were assessed by ABR recording. The average hearing thresholds to pure tone and click stimulation are shown in Fig. 6. The hearing thresholds measured before and 2 mo after the surgery are almost identical within the whole frequency range 1–32 kHz ($P = 0.886$, two-way ANOVA).

Distortion-Product Otoacoustic Emissions (DPOAEs)

The DP-grams (function of the DPOAE amplitudes above background noise on increasing frequency stimuli) were constructed from individual ear DPOAE recordings. Average DP-grams obtained from the left (operated) and right (non-operated) ears are shown in Fig. 7. Average DP-grams obtained from both ears before surgery are almost identical ($P = 0.128$, two-way ANOVA); further, the average DP-grams from left (operated) and right (non-operated) ears 2 mo after surgery did not differ from those measured before surgery ($P = 0.624$ left ear, $P = 0.443$ right ear; two-way ANOVA) (Fig. 7a, b, respectively).

Radiological Evaluation

In the control group, the "hot spot" bone densities of implanted material were estimated in 920 to 1300 HU (*mean* =1050 HU) and areal bone densities in 630 to 850 HU (*mean* =780 HU). Thickening of the middle ear mucosa was observed in 3 animals; regardless, all animals had aerial tympanic bulla without effusion in the middle ear. CT scans did not show any pathological changes in the inner ear.

In the 1 M group, the "hot spot" bone densities of implanted material with hBM-MSCs were of 800 to 1100 HU (*mean* =980 HU) and areal bone densities of 540 to 800 HU (*mean* =720 HU). Compared to the control group, neither the "hot spot" densities nor the areal bone densities were significantly different (Table 2). Thickening of the middle ear mucosa was observed in only one animal. All animals had aerial tympanic bulla without effusion in the middle ear. CT scan did not show any pathological changes in the inner ear.

However, bone densities were higher in the 2 M group with "hot spot" values of 850 to 2100 HU (*mean* =1640 HU) and areal bone densities of 650 to 1950 HU (*mean* =1470 HU).

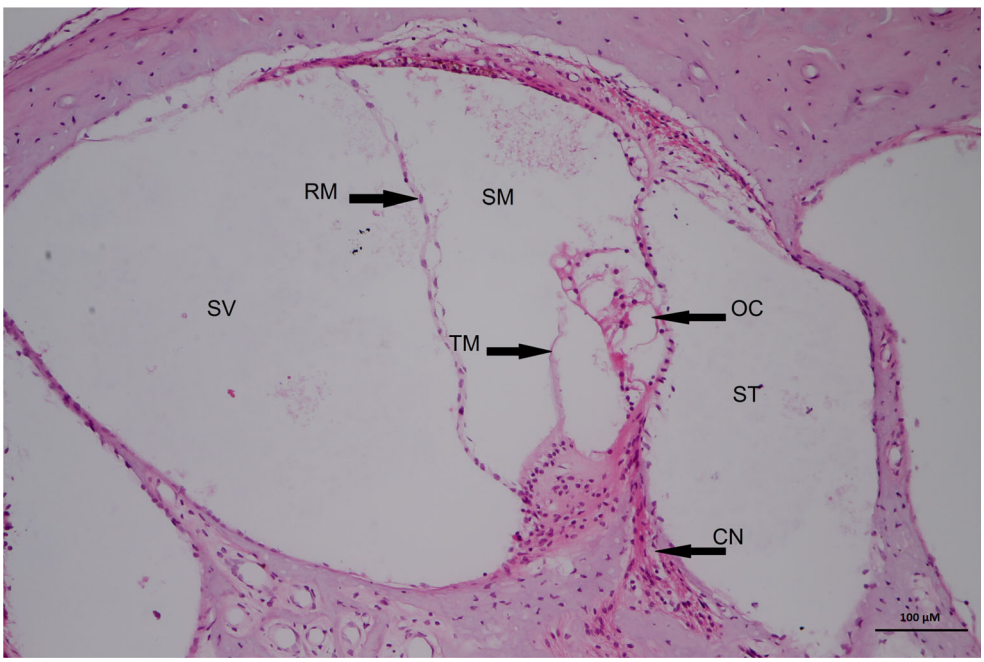

Fig. 4 Histological examination of the cochlea 60 days after implantation of the biomaterial seeded with hBM-MSCs (decalcification; Haematoxylin-eosin; scale bar 100 µm). SV – Scala vestibuli; SM - Scala media; ST – Scala tympani; OC - Organ of Corti; RM – Reissner's membrane; TM – Tectorial membrane; SV – Stria vascularis; CN - Cochlear nerve fibres

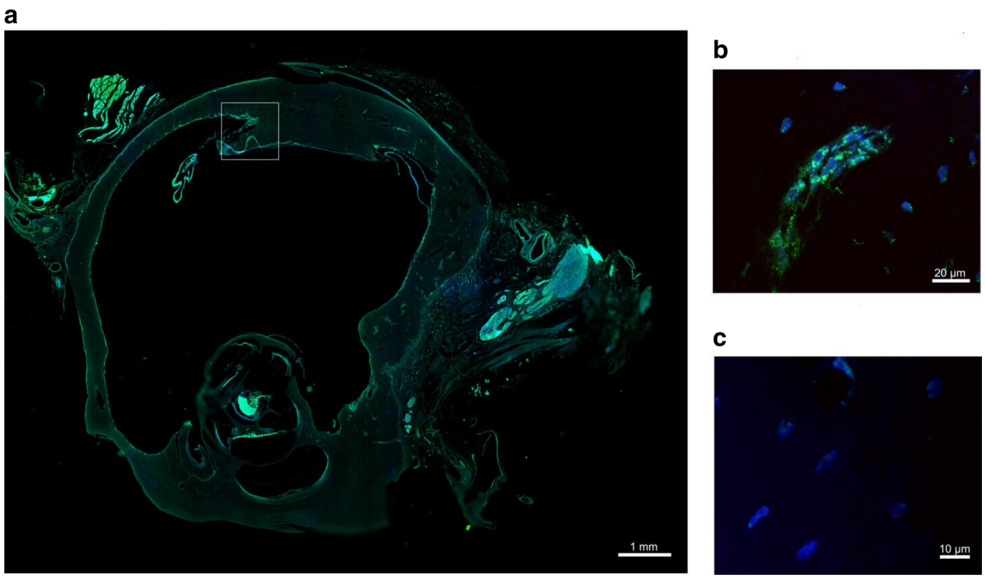

Fig. 5 Immunodetection of hMSCs with anti-MTCO2 antibodies. $MTCO2^+$ cells (green; DAPI, blue) can be observed at the site lesion in the tympanic bulla 60 days after surgery (initial transplant of 5×10^6 hBM-MSCs). **a** The lesion site is completely healed (full section), the white square shows part of the lesion with implanted with the osteoconductive material (CEM-OSTETIC®) and hMSCs; scale bar 1 mm. **b** $MTCO2^+$ staining within the lesion site; scale bar 20 μm. **c** $MTCO2^-$ staining control; scale bar 10 μm

Both of these values were significantly higher when compared to the control and 1 M groups (Table 2). Thickening of the middle ear mucosa was observed in 2 animals, with thickening of tympanic membrane observed in one of them. All animals had aerial tympanic bulla without effusion in the middle ear. CT scan did not show any pathological changes in the inner ear (Fig. 8a, b).

Discussion

Occasionally, middle ear cholesteatoma surgery requires a canal wall down (CWD) mastoidectomy; this approach is very effective in the treatment of cholesteatoma although with the downside of inflicted changes to the anatomy of the external and middle ear; further, the ear canal loses its self-clearing ability and the exteriorized mastoid cavity becomes the target of chronic infections. Moreover, temporal bone reconstruction after middle ear surgery is still a difficult task; in addition, the

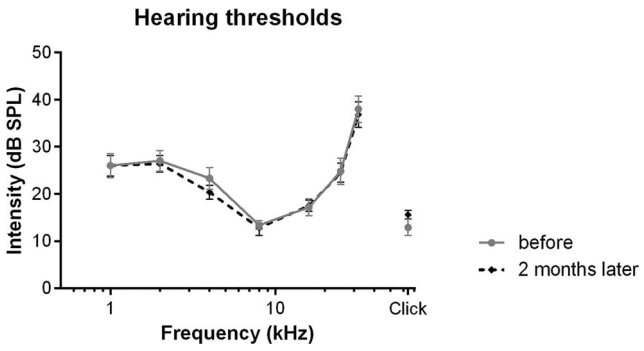

Fig. 6 Average hearing thresholds assessed on the basis of ABR recording to pure tone and click stimulation measured before and 2 mo after surgery. Error bars represent ± SEM. $p \leq 0.05$ was considered to be significant

patients need regular treatment to clear any keratin debris, have bathing restrictions, a poor fit for hearing aids, and recurrent ear discharge. Some of these cavity problems have been diminished by the obliteration technique, which only reduces the size of the mastoid cavity. Regardless, no surgical technique is able to provide a complete closure of the mastoid cavity nor the anatomy normalization of the middle and external ear [13, 24–27].

The considerable potential of MSCs in the regeneration and replacement of damaged or lost bone tissue hints at a promising approach to reconstructive surgery after CWD mastoidectomy. Such potential has been previously shown in several studies [10, 28]; however, compared to other bone defect locations the middle ear is a relatively nuanced one. The otologists find themselves reconstructing bone of a particular shape between an air cavity and soft tissues, able to preserve the function and aeration of the middle ear cavity. Concerning MSCs delivery, a common approach consists in the direct injection of these cells suspended in saline buffer into the damaged tissue [29]; unfortunately, this procedure has proven to be inadequate in temporal bone reconstruction. Therefore, a solid and elastic scaffold able to be fixed in the proper location is needed to correct such bone defects; further, such scaffold should facilitate osteogenesis.

In this regard, Jang et al. reported the improved bone formation effect of a polycaprolactone scaffold combined with human umbilical cord serum or beta tricalcium phosphate [30]; and Kim et al. showed a higher bone formation along the periphery of a mastoid bulla defect using human ear adipose-derived stromal cells in combination with a polycaprolactone scaffold and osteogenic differentiation medium [28]. We opted instead for a hydroxyapatite scaffold combined with tissue glue because of its excellent biocompatibility and osteoconductive potential, the combination of

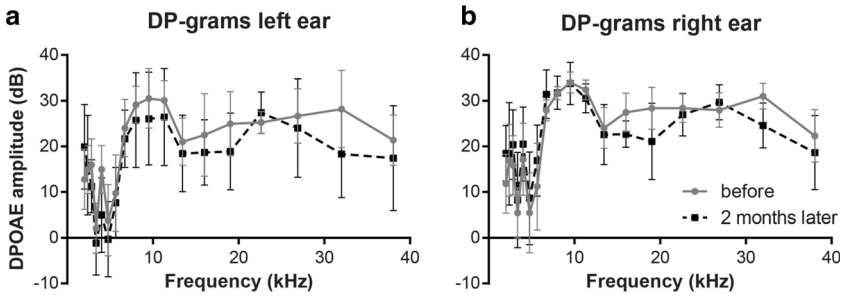

Fig. 7 The average DP-grams (the function of the DPOAE amplitudes above background noise on increasing frequency stimuli) measured before and 2 months after surgery in the left (operated) (**a**) and right (non-operated) ears (**b**). Error bars represent ± SEM. $p \leq 0.05$ was considered to be significant

tissue glue provides favourable mechanical properties when fixing the material into the defect, resulting in the adequate reconstruction of new bone between the air tympanic cavity and soft tissues. The shape and position of the new bone formation was achieved successfully, as proven by a HRCT scan followed by tympanic bulla exploration, also with satisfactory anatomical results of MSC implantation. Elaborating further, the new bone formation closed the tympanic bulla, possessed the proper shape, and showed no apparent morphological abnormalities or functional consequences. To effectively distinguish the effect of MSCs, we compared the osteoneogenic capacity of the biomaterial with and without MSCs, observing a significantly higher osteoneogenic capacity in the presence of MSCs.

Although past studies have focused on temporal bone reconstitution using MSCs, the data concerning middle ear changes and functional consequences of the treatment was lacking [11, 28, 30]. Because any changes in the small tympanic cavity or inner ear could deteriorate hearing, we tested the hearing capacity of the subjects using two methods of objective audiometry: The test of outer hair cells in the cochlea was evaluated by distortion-product otoacoustic emissions (DPOAEs), whereas the hearing threshold was assessed by auditory brainstem response recordings (ABRs). Both methods are sensitive to any changes in the tympanic membrane or to middle ear discharge; however, neither middle ear discharge nor tympanic membrane perforations were found in our experimental groups, although one animal showed CT signs of tympanic membrane thickening and was excluded from inner ear hearing tests.

DPOAEs are generated when the cochlea is simultaneously stimulated by two pure tone frequencies, its prevalence is of 100% in normal hearing and the response from both ears should be correlated. In guinea pigs, DPOAEs can be recorded separately for each ear allowing a hearing test comparison between the experimental (left) and control (right) ears. DPOAEs response are shown in a DP-gram modality; it must be highlighted that no significant difference in DPOAEs could be observed between the 2 M and control groups ($p<0.05$).

An ABR is a synchronous neural response to an auditory stimulus, it is used as an objective method estimating hearing sensitivity. In guinea pigs, ABRs are measured as a bilateral hearing threshold evaluated after 2 months of MSCs implantation. In comparison with preoperative hearing, no significant ABR shift could be observed in the evaluated animals ($p<0.05$); further, neither ABRs or DPOAEs revealed any evidence of MSCs induced ototoxicity in the middle ear.

The presence of an inflammatory response was examined by HRCT scans, clinical exploration of the tympanic bulla, and histological examination. No inflammatory response could be observed around the implanted material nor in the middle ear, and macroscopic exploration of the tympanic bulla confirmed the firm occlusion of the operative defect in the anterior wall of the bulla in all cases. Further, middle ear infections are commonly manifested by middle ear secretion; however, the CT scans of the experimental animals did not reveal any secretion in the aerial tympanic bulla. Furthermore, an indirect indication of middle ear inflammation is manifested by the thickening of the middle ear mucosa which was unchanged in the majority of the tested animals (6 out of 7, and 5 out of 8 in the control and experimental groups, respectively). The histological analysis confirmed minimal changes in hearing thresholds and otoacoustic emissions. However, the immunohistochemical evaluation revealed a significantly higher distribution of $CD3^+$ T-lymphocytes in the experimental group 1 M in comparison with the control group, with

Table 2 HRCT of the temporal bone transplanted with osteoconductive material (CEM-OSTETIC ®) seeded with 5×10^6 cells hBM-MSCs. Data shown describe the mean ratio (range of minimal and maximal). P_1 - control vs 1 M; P_2 - control vs 2 M; P_3 - 1 M vs 2 M. $p \leq 0.05$ was considered to be significant

	Minimal	Maximal	Mean	
Hot spots density (control group)	920	1300	1050	
Area density (control group)	630	850	780	
Hot spots density (group 1 M)	800	1100	980	P_1 = NS
Area density (group 1 M)	540	800	720	
Hot spots density (group 2 M)	850	2100	1640	P_2 = 0.0203
Area density (group 2 M)	650	1950	1470	P_3 = 0.0177

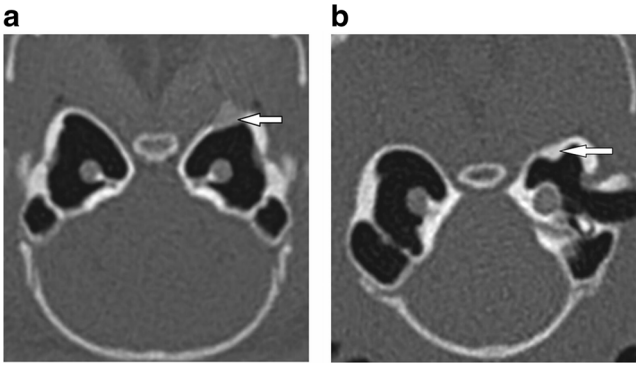

Fig. 8 Radiological examination of the Guinea pig's head by HRCT at the level of the tympanic bulla. The arrow shows the CEM-OSTETIC® scaffold seeded with hBM-MSCs (5×10^6 cells) transplanted into the bone defect. **a** The "hot spots" density in the implanted material is of 1100 HU (areal density of 850 HU) in the 1 M group, whereas in the 2 M group (**b**), the "hot spots" density of the implanted material is of 1800 HU (areal density of 1660 HU)

$TRAP^+$ macrophages present in all specimens. The migration of T lymphocytes and macrophages could be due to the paracrine effect of MSCs facilitating osteogenesis as it is known that MSCs have the ability to inhibit or activate certain immune cells thus affecting the overall response to tissue injury and the repair processes [31]. It must be mentioned that an adverse inflammatory response caused by neutrophils could damage the implanted material and impair bone reconstruction; however, we did not detect any CHAE positive cells (neutrophils) in the analysed specimens.

Recent studies, reviewed by Pacini and Petrini [32], have reported considerable progress in tissue regeneration driven by MSCs therapy, with recent data indicating the residing anatomical location of MSCs in the "perivascular" space of blood vessels dispersed across the whole body. This in turn suggests that MSCs contributes to the formation of new blood vessels in vivo as MSCs are known to release angiogenic factors facilitating blood vessel formation in vitro [32]. Often, the lack of new blood vessels is responsible for the failure of bone repair applications because of insufficient nutritional support to the bone graft [33]; therefore, early vascularization driven by the angiogenic effect of MSCs ensures an ingrowth of osteogenic reparative cells within an implanted composite in critical bone defects. Sure enough, we detected angiogenesis "hot spots" as small blood vessel lumina delineated by $CD31^+$ endothelial cells in our experimental subjects, showing a higher number of small blood vessels in the 1 M group when compared to control group; however, the difference was not significant despite the median of small vessels in the experimental group being two times higher than in the control (13 versus 7 in area of 0.283 mm^2).

The osteogenic capacity of MSCs has been reported in several studies [11, 28, 30, 34]; however, it was unknown whether this effect was due to the persisting presence of the implanted MSCs or to the effect of bioactive molecules secreted from dead cells in our model. To answer this question, primary antibodies targeting human cytochrome C oxidase subunit II (MTCO2) were used to determine the presence of implanted hBM-MSCs in the ears of the treated guinea pigs, finding the presence of these cells in 88 and 67% cases of the specimens after one and 2 mo after MSCs implantation, respectively. Apparently, the developed implantation technique of hBM-MSCs on hydroxyapatite scaffolds enables cell survival for at least 2 months.

The reconstruction of temporal bone defects after operative trauma is still a clinical challenge and the use of cell-based therapies represents one of the most advanced methods in enhancing a regenerative response. In the present study, we managed to reconstruct the middle ear wall bone, achieving the satisfactory shape and position of the new bone formation and preserving hearing capacity. Taken together, the present results confirm the positive effect of hBM-MSCs on temporal bone reconstruction in a Guinea pig model.

Conclusion

Our study reveals the ability of hydroxyapatite scaffolds seeded with hBM-MSCs to regenerate temporal bone defects and to restore full hearing capacity, comparable to preoperative levels, in the treated subjects. Therefore, we consider this approach as an effective alternative in the treatment of temporal bone bone defects following middle ear surgery due to cholesteatoma.

Acknowledgments This work was supported by grants MH CZ-DRO (UHHK, 00179906) and PROGRES Q40/6. The authors wish to thank Dr. Daniel Díaz, Ph.D. for his kind assistance in English language revision and proofreading of this manuscript.

Compliance with Ethical Standards

Conflicts of Interest The authors declare no conflicts of interest.

References

1. Franco-Vidal, K., Daculsi, G., Bagot d'Arc, M., Sterkes, O., Smail, M., Robier, A., Bordure, P., Claros, P., Paiva, A., Darrouzet, V., Anthoine, E., & Bedear, J. P. (2014). Tolerance and osteointegration of TricOs(TM)/MBCP(®) in association with fibrin sealant in mastoid obliteration after canal wall-down technique for cholesteatoma. *Acta Oto-Laryngologica, 134*(4), 358–365.
2. Suzuki, H., Ikezaki, S., Imazato, K., Koizumi, H., Ohbuchi, T., Hohchi, N., & Hashida, K. (2014). Partial mastoid obliteration combined with soft-wall reconstruction for modele ear cholesteatoma. *Annals of Otology, Rhinology and Laryngology, 123*(8), 571–575.
3. Harris, A. T., Mettias, B., & Lesser, T. H. (2016). Pooled analysis of the evidence for open cavity, combined approach and

reconstruction of the mastoid cavity in primary cholesteatoma surgery. *Journal of Laryngology and Otology, 130*(3), 235–241.
4. Seong, J. M., Kim, B. C., Park, J. H., Kwon, I. K., Mantalaris, A., & Hwang, Y. S. (2010). Stem cells in bone tissue engineering. *Biomedical Materials, 5*(6), 062001. https://doi.org/10.1088/1748-6041/5/6/062001.
5. Gamie, Z., MacFarlane, R. J., Tomkinson, A., Moniakis, A., Tran, G. T., Gamie, Y., Mantalaris, A., & Tsiridis, E. (2014). Skeletal tissue engineering using mesenchymal or embryonic stem cells: clinical and experimental data. *Expert Opinion on Biological Therapy, 14*(11), 1611–1639.
6. Dominici, M., Le Blanc, K., Mueller, I., Slaper-Cortenbach, I., Marini, F., Krause, D., Deans, R., Keating, A., Prockop, D. J., & Horwitz, E. (2006). Minimal criteria for defining multipotent mesenchymal stromal cells. The International Society for Cellular Therapy position statement. *Cytotherapy, 8*(4), 315–317.
7. Fernández Vallone, V. B., Romaniuk, M. A., Choi, H., Labovsky, V., Otaegui, J., & Chasseing, N. A. (2013). Mesenchymal stem cells and their use therapy: what has been achieved? *Differentiation, 85*(1–2), 1–10.
8. Frölich, K., Scheryed, A., Mlynski, R., Technau, A., Hagen, R., Kleinsasser, N., & Radeloff, A. (2011). Multipotent stromal cells for autologous cell therapy approaches in the Guinea pig model. *Journal for Oto-Rhino-Laryngology and its Related Specialties, 73*(1), 9–16.
9. Peng, H., Ming, L., Yang, R., Liu, Y., Liang, Y., Zhao, Y., Jin, Y., & Deng, Z. (2013). The use of laryngeal mucosa mesenchymal stem cells for the repair the vocal fold injury. *Biomaterials, 34*(36), 9026–9035.
10. Skoloudik, L., Chrobok, V., Kalfert, D., Koci, Z., & Filip, S. Multipotent mesenchymal stromal cells in otorhinolaryngology. *Medical Hypotheses, 82*(6), 769–773.
11. Skoloudik, L., Chrobok, V., Kalfert, D., Koci, Z., Sykova, E., Chumak, T., Popelar, J., Syka, J., Laco, J., Dedkova, J., Dayanithi, G., & Filip, S. (2016). Human multipotent mesenchymal stroma cells in the treatment of postoperative temporal bone defect: an animal model. *Cell Transplantation, 25*(7), 1405–1414.
12. Tuček, L., Kočí, Z., Kárová, K., Doležalová, H., & Suchánek, J. (2017). The osteogenic potential of human nondifferentiated and pre-differentiated mesenchymal stem cells combined with an osteoconductive scaffold – early stage healing. *Acta Medica (Hradec Králové), 60*(1), 12–18.
13. Murray, B., & Wilson, D. J. (2001). A study of metabolites as intermediate effectors in angiogenesis. *Angiogenesis, 4*(1), 71–77.
14. Boomsma, R. A., & Geenen, D. L. (2014). Mesenchymal stem cells secrete multiple cytokines that promote angiogenesis and have contrasting effects on chemotaxis and apoptosis. *PLoS One, 7*(4), e35685. https://doi.org/10.1371/journal.pone.0035685.
15. Amiri, F., Jahanian-Najafabadi, A., & Roudkenar, M. H. (2015). In vitro augmentation of mesenchymal stem cells viability in stressful microenvironments: In vitro augmentation of mesenchymal stem cells viability. *Cell Sterss and Chaperones, 20*(2), 237–251.
16. Luo, H., Zhang, Y., Zhang, Z., & Jin, Y. (2012). The protection of MSCs from apoptosis in nerve regeneration by TGFβ1 through reducing inflammation and promoting VEGF-dependent angiogenesis. *Biomaterials, 33*(17), 4277–4287.
17. Madrigal, M., Rao, K. S., & Riordan, N. H. (2014). A review of therapeutic effects of mesenchymal stem cell secretions and induction of secretory modification by different culture methods. *Journal of Translational Medicine, 12*, 260. https://doi.org/10.1186/s12967-014-0260-8.
18. Singh, J., Onimowo, J. O., & Khan, W. S. (2015). Bone marrow derived stem cells in trauma and ortophedics: a review of the current trend. *Current Stem Cell Research and Therapy, 10*(1), 37–42.
19. Bortolotti, F., Ukovich, L., Razban, V., Martinelli, V., Ruozi, G., Pelos, B., Dore, F., Giacca, M., & Zaschigna, S. (2015). In vivo therapeutic potential of mesenchymal stromal cells depends on the source and the isolation procedure. *Stem Cell Reports, 4*(3), 332–339.
20. Squillaro, T., Peluso, G., & Galderisi, U. (2016). Clinical trials with mesenchymal stem cells: an update. *Cell Transplantation, 25*(5), 829–848.
21. Vanecek, V., Klima, K., Kohout, A., Foltan, R., Jirousek, O., Sedy, J., Stulik, J., Sykova, E., & Jendelova, P. (2013). The combination of mesenchymal stem cells a bone scaffold in the treatement of vertebral body defects. *European Spine Journal, 22*(12), 2777–2786.
22. Wysocki, J. (2005). Topographical anatomy of the Guinea pig temporal bone. *Hearing Reserach, 199*(1–2), 103–110.
23. Truncova, K., Ruyickova, K., Vanecek, V., Sykova, E., & Jendelova, P. (2009). Properties and growth of human bone marrow mesenchymal stromal cells cultivated in different media. *Cytotherapy, 11*(7), 874–885.
24. Leatherman, B. D., & Dornhoffer, J. L. (2002). Bioactive glass ceramic particles as an alternative for mastoid obliteration: results in an animal model. *Otology and Neurotology, 23*(5), 657–660.
25. Mendez-Ferrer, S., Michurina, T. V., Ferrari, F., Maylom, A. R., Macarthur, B. D., Lira, S. A., Scadden, D. T., Ma'ayan, A., Enikopolov, G. N., & Frenette, P. S. (2010). Mesenchymal and hematopoietic stem cells from a unique bone marrow niche. *Nature, 466*(7308), 829–834.
26. Lee, H. B., Lim, H. J., Cho, M., Yang, S. M., Park, K., Park, H.-Y., & Choung, Y. H. (2013). Clinical significance of β-tricalcium phosphate and polyphosphate for mastoid cavity obliteration during middle ear surgery: human and animal study. *Clinical and Experimental Otorhinolaryngology, 6*(3), 127–134.
27. Murray, I. R., West, C., Hardy, W. R., James, A. W., Park, T. S., Nguyen, A., Tawonsawatruk, T., Lazzari, L., Soo, C., & Péault, B. (2014). Natural history of mesenchymal stem cells, from vessel walls to culture vessel. *Cellular and Molecular Life Sciences, 71*(8), 1353–1374.
28. Kim, Y. J., Park, S. G., Shin, B., Kim, J., Kim, S. W., Choo, O. S., Yin, X. Y., Min, B. H., & Choung, Y. H. (2017). Osteogenesis for postoperative temporal bone defects using human ear adipose-derived stromal cells and tissue engineering: an animal model study. *Journal of Biomedical Materials Research A, 105*(12), 3493–3501.
29. Kashiwa, K., Kotobiki, N., Tadokoro, M., Matsumura, K., Hyon, S. H., Yoshiya, S., & Ohgushi, H. (2010). Effects of epigalloctechin gallate on osteogenic capability of human mesenchymal stem cells after suspension in phosphate-buffered saline. *Tissue Engineering Part A, 16*(1), 91–100.
30. Jang, C. H., Cho, Y. B., Choi, C. H., Jang, Y. S., Jung, W. K., Lee, H., & Kim, G. H. (2014). Effect of umbilical cord serum coated 3D PCL/alginate scaffold for mastoid obliteration. *International Journal Pediatric Otorhinolaryngology, 78*(7), 1061–1065.
31. Kaplan, J. M., Youd, M. E., & Lodie, T. A. (2011). Immunomodulatory activity of mesenchymal stem cells. *Current Stem Cell Research and Therapy, 6*(4), 297–316.
32. Pacini, S., & Petrini, I. (2014). Are MSCs angiogenic cells? New insights on human nestin-positive bone marrow-derived multipotent cells. *Frontiers in Cell Developmental Biolology, 2*. https://doi.org/10.3389/fcell.2014.00020.
33. Seebach, C., Henrich, D., Wilhelm, K., Barker, J. H., & Marzi, I. (2012). Endothelial progenitor cells improve directly and indirectly early vascularization of mesenchymal stem cell derived bone regeneration in a critical bone defect in rats. *Cell Transplantation, 21*, 1667–1677. https://doi.org/10.3727/096368912X638937.
34. Camernik, K., Barlic, A., Drobnic, M., Marc, J., Jeras, M., & Zupan, J. (2018). Mesenchymal stem cells in the musculoskeletal system: from animal models ti human tissue regeneration? *Stem Cell Reviewes and Reports*. https://doi.org/10.10007/s12015-018-9800-6.